Research Square

Preprints are preliminary reports that have not undergone peer review.
They should not be considered conclusive, used to inform clinical practice,
or referenced by the media as validated information.

The hydrocarbon enrichment characteristics of the AD well area in Tahe Oilfield, Tarim Basin China

Yongqiang Li

liyongqiangz@163.com

Petroleum Exploration and Production Research Institute

Liying Cao

Petroleum Exploration and Production Research Institute

Dong Han

Petroleum Exploration and Production Research Institute

Research Article

Keywords: Tahe Oilfield, AD well area, Ordovician reservoir, fault development characteristics, fracture-cavity characteristics, hydrocarbon enrichment

Posted Date: November 9th, 2026

DOI: https://doi.org/10.21203/rs.3.rs-11275888/v1

License: This work is licensed under a Creative Commons Attribution 4.0 International License.
Read Full License

Additional Declarations: No competing interests reported.

The hydrocarbon enrichment characteristics of the AD well area in Tahe Oilfield, Tarim Basin China

Yongqiang Li[1]*, Liying Cao[1], Dong Han[1]

1 Petroleum Exploration and Production Research Institute, Sinopec, Beijing 10083, China

*Communication author

Abstract: In response to challenges such as poor identification of low-order faults with weak activity and insufficient understanding of fracture-cavity genetic mechanisms and hydrocarbon enrichment patterns in the fault-controlled karst area of western Tahe Oilfield, this study investigates the development characteristics of faults and fracture-cavity systems, as well as their control on hydrocarbon enrichment. Research indicates that enhancing seismic imaging accuracy through multi-scale filtering can effectively identify low-order faults that are undetectable by conventional seismic attribute analysis. Based on the genetic mechanisms and activity periods of faults, they are classified into three categories. The newly identified NE-trending low-order faults are classified as second-order faults and possess certain hydrocarbon charging capabilities. Controlled by faults and unconformities, fracture-cavity systems are distributed in both shallow and deep layers. In the eastern and western regions, vertical dissolution dominated by fault-controlled is predominant, while the central area exhibits a combination of fault-controlled vertical dissolution and layer-controlled karst conduits. Based on the oil-water distribution characteristics observed in actual drilling, two hydrocarbon enrichment and high-productivity models have been established: 1) NE-trending fault-controlled vertical charging and enrichment along source-connected faults, and 2) lateral charging and enrichment controlled by secondary faults in sandwiched zones. Through hydrocarbon enrichment assessment, both models can be extended from conventional secondary fault-controlled areas to unexplored low-order fault zones, and from shallow layers to unexplored deep formations. The success of appraisal wells has confirmed this understanding, which provides important guidance for the effective development of unproduced reserves in Tahe Oilfield.

Keywords: Tahe Oilfield, AD well area, Ordovician reservoir, fault development characteristics, fracture-cavity characteristics, hydrocarbon enrichment

1 Introduction

The differential enrichment pattern of oil and gas, common in various reservoir types, which determines the deployment direction of hydrocarbon development potential and is closely related to factors such as hydrocarbon charging adjustment and the development characteristics of reservoir bodies. Examples include the Permian Basin in West Texas, USA; deepwater oil and gas fields in East Africa; the Pre-Caspian condensate gas fields (Punaova & Vinogradova 2010; Cai et al. 2020; Fairhurst et al. 2021); as well as China's Longwangmiao Gas Reservoir in central Sichuan, the Huanghua Depression, and the Ordovician reservoirs in the Shunbei area (Liu et al.2015; Tian et al.2021; Lin et al.2022). As the most typical karst fracture-cavity reservoir in China, the Tahe Oilfield in the Tarim Basin exhibits a geological framework where faults serve as the primary pathways for hydrocarbon migration and adjustment, while karst fracture-cavity units act as the main reservoirs for hydrocarbon accumulation. The interplay between these two factors collectively determines the extent of hydrocarbon enrichment. The AD well area is located in the fault-controlled karst area of the western slope of the Tahe Oilfield, where multiple sets of NE- and NW-trending strike-slip faults have developed. The overall degree of hydrocarbon enrichment is controlled by the NE-trending faults and the associated fracture-cavity systems. The local fault activity in the region is weak, with poor identification of low-order faults and an unclear distribution pattern of karst fracture-cavity systems. As a result, the understanding of hydrocarbon enrichment patterns controlled by faults and karst processes remains inadequate. Based on this, this paper integrates seismic attribute extraction to conduct comprehensive research on fault analysis, fracture-cavity characterization, and hydrocarbon enrichment evaluation, aiming to provide new insights into the high-yield enrichment patterns and further development potential deployment in the AD well area.

2 Geological Background

The Tahe Oilfield is located on the slope belt of the Akekule Arch in the southern wing of the Shaya Uplift, within

the northern depression of the Tarim Basin. It is bounded by the Hanikatam Depression to the west, the Caohu Depression to the east, the Manjiaer Depression to the south, and the Yakela Faulted Arch to the north (Fig.1; Zhang 1999). The Ordovician system comprises six stratigraphic units: the Penglaiba, Yingshan, Yijianfang, Qiaerbake, Lianglitage, and Sangtamu formations. Among these, the Yijianfang and Yingshan formations are the primary layers for karst reservoir development in the Tahe Oilfield. These formations were deposited in an open-platform to platform-slope environment, dominated by thick limestone lithology (Liu 2002).

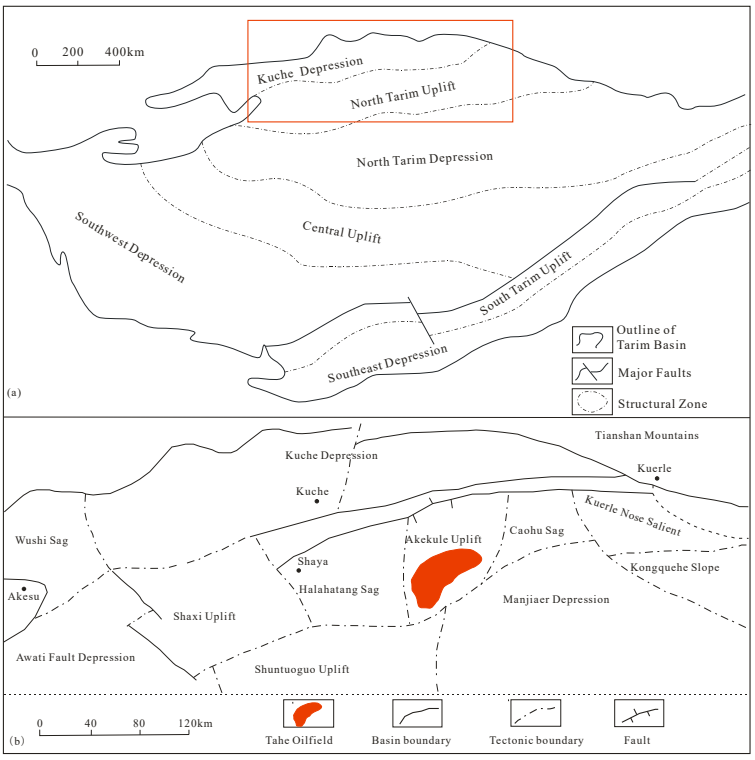


Fig.1 Tectonic framework and location of the study area

a. Tectonic unit map of Tarim Basin; b. Location map of Tahe Oilfield

The Akekule Arch is a long-term paleo-arch developed on a Pre-Sinian metamorphic basement, having undergone multiple phases of tectonic movement and deformation superposition, including the Caledonian, Hercynian, Indosinian-Yanshanian, and Himalayan periods (Li & Fan 2011). Among these, the intense tectonic activity during the early Hercynian period caused crustal uplift, forming numerous folds and faults while subjecting the Ordovician strata to certain degrees of erosion, resulting in a regional unconformity surface. Near the unconformity surface in the eroded area, strata

experienced strong erosion, forming a spatial network system that expanded the dissolution area of meteoric water, creating a karst system conducive to karst development. This led to the formation of a large unconformity-karst fracture-cavity reservoir characterized by extensive contiguous oil-bearing zones with uneven oil distribution. In the covered area, the relatively low permeability of the carbonate matrix itself hinders large-scale fluid inflow and outflow, thereby limiting dissolution and reservoir improvement. However, the developed NE- and NNW-trending fault sets form a networked fault system that constrains fluid movement directions, increases the contact area between water and carbonate rocks, expands the dissolution range of surface and groundwater, enhances carbonate permeability, and accelerates dissolution rates. This not only further enlarges pre-existing dissolution pores and caves but also generates new dissolution voids. The fractures and damaged zones formed by fault activity exhibit good connectivity, improving reservoir physical properties and promoting the development and evolution of karst, and ultimately creates favorable reservoir spaces known as fault-controlled karst reservoirs. The AD well area belongs to a fault-controlled karst setting within the covered area, where faults control the development of fracture-cave systems and hydrocarbon enrichment.

3 Data and Methodology

This study focuses on the AD well area in Tahe Oilfield. The dataset includes well log interpretation and production data from 56 wells, as well as 180 km² of 3D seismic data (with a sampling interval of 1 ms and a grid size of 15×15 m). The hydrocarbon enrichment patterns are summarized based on three aspects: fault-related hydrocarbon charging capacity, reservoir distribution, and high-production characteristics of drilled wells. (1) Special seismic processing techniques were applied to enhance the imaging precision of seismic data. Coherence attributes, reflecting the degree of fracturing, were extracted to identify faults at various scales. Subsequently, the genesis and activity phases of these faults were analyzed. Faults were classified based on three criteria: scale of fault activity, depth of fault penetration, and the correlation between fault activity phases and hydrocarbon accumulation periods. The hydrocarbon charging capacity of faults at different levels was determined by analyzing their strike, connectivity to source rocks, and intensity of late-stage activity. (2) Fracture-

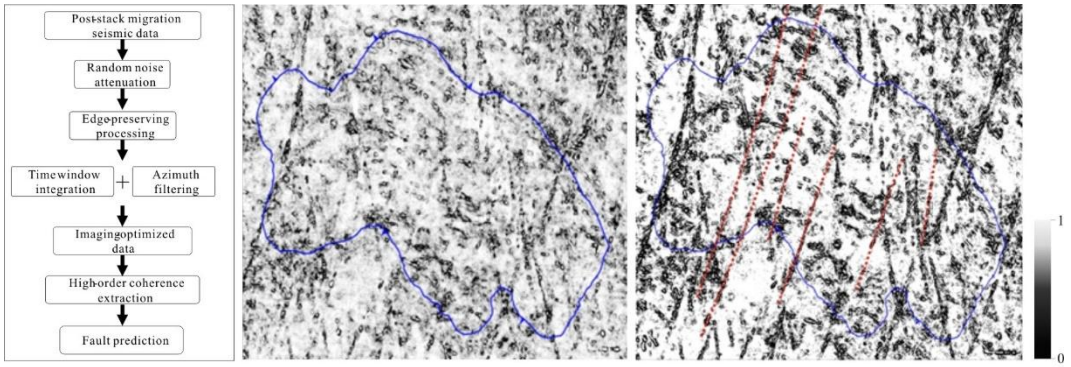
cavity systems were characterized using seismic attributes. The genesis of karst features was analyzed based on controlling factors such as paleo-topography, faults, and paleo-drainage systems. Finally, the spatial distribution characteristics of different types of fracture-cavities were determined. (3) The oil-water distribution characteristics of drilled wells were analyzed to summarize the features of high-production wells in terms of fault charging and fracture-cavity distribution. A model for high-yield hydrocarbon enrichment was established. This model was used to identify future developed targets and guide well placement in the study area.

4 Fault Development Characteristics

4.1 Fault Identification Based on Multi-scale Filtering Processing

Low-order faults are characterized by their small scale and inconspicuous displacement. Simultaneously, due to significant burial depth of the strata and reduced seismic resolution, conventional seismic methods often fail to identify them clearly. By optimizing seismic imaging processing methods, we aim to minimize the effects of noise interference and random stratigraphic jitter as much as possible, thereby highlighting the stratigraphic dislocation response caused by the development of low-order faults. ① Dip-Angle Fault Enhancement Processing Based on Noise Reduction. This process improves the signal-to-noise ratio. The objective is to remove noise while preserving the edges of seismic data, emphasizing the combination of noise suppression and enhancement. It increases the recognizability of local structures, highlights fault reflection characteristics, and further improves fault visibility. ② Imaging Optimization Based on Time-Window Integration + Azimuth Scanning. Seismic data undergoes integration within specific vertical time windows to counteract variations caused by stratigraphic jitter within the window. Data integration often increases low-frequency components and rotates the phase by -90 degrees. While this integration may reduce resolution, it enhances the detection of anomalous stratigraphic dislocations that cut through multiple seismic events. After optimized seismic imaging, high-frequency noise in seismic profiles is significantly reduced, stratigraphic continuity is improved, and the seismic response at event discontinuities is enhanced to some extent. Based on the optimized data, extracting high-order coherence attribute

volumes reveals clearer fault geometries and significantly improved continuity in coherence profiles. Additionally, it highlights the stratigraphic dislocation response caused by low-order fault development, effectively achieving accurate characterization of low-order faults (Fig.2).



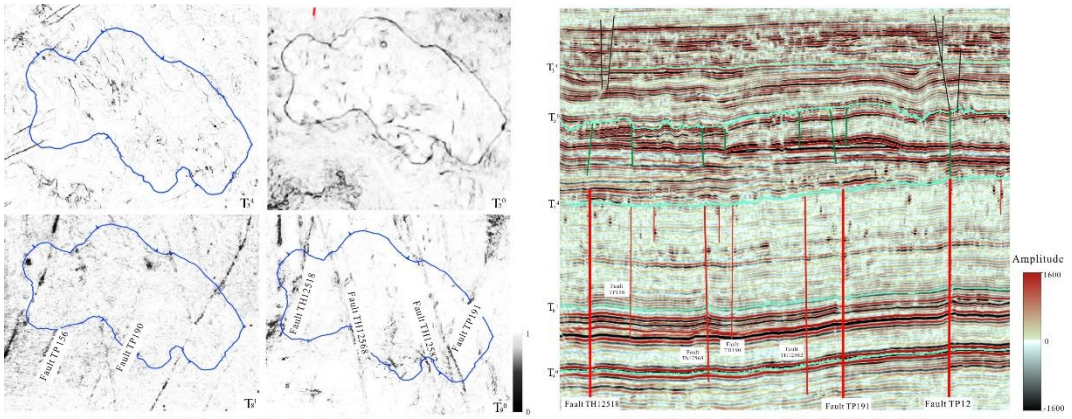
a.Fault Prediction Workflow Based on Multi-scale Filtering b. Coherence Attribute Map Before Multi-scale Filtering Processing c. Coherence Attribute Map After Multi-scale Filtering Processing

Fig. 2 Planar View of Seismic Coherence Attribute for Interval T76 Lower 0-10 ms in AD Well area

4.2 Fault Genetic Mechanism

The study area has undergone multiple tectonic movements, including the Caledonian, Hercynian, Indosinian–Yanshanian, and Himalayan orogenies, resulting in the formation of a multi-stage, superimposed fault system with fractures of varying orders (Zhang et al, 2020). During the Caledonian period, under sustained N-S oriented compressive stress, a conjugate strike-slip fault system developed under a pure shear stress regime. The slip of conjugate blocks was constrained, leading to the development of NE and NW trending small to medium scale fractures resembling a conjugate pattern within the blocks. Controlled by local stress fields, NWW trending transfer faults formed between the NE-trending fractures. In the Hercynian period, the maximum principal stress direction gradually shifted, with dominant activity along NNE trending faults. Due to the coverage of salt bodies, the overlying en echelon faults terminated at the salt boundaries. From the Indosinian to Himalayan period, the orientation of the maximum principal stress further rotated, reactivating the NNE trending faults with dextral strike-slip motion. Drag shear associated with this movement led to the development of a series of NE trending en echelon faults (Fig.3a) Under continued N–S compression, numerous NNE and NNW trending joints propagated and linked, forming conjugate strike-slip faults under pure shear. Faults TH12518 and TP191 remained active from the Caledonian through the Yanshanian–Himalayan period. The NE, NW, and NWW trending faults confined between

them showed localized activity after the mid to late Hercynian, while internal faults within the block exhibited no significant activity during the Hercynian (Fig 3b).



a.Coherence slice of key horizons b.Typical seismic profiles of multi-stage faults

Fig 3. Coherence slices and typical seismic profiles of multi-stage faults.

4.3 Fault Hierarchy Classification

The classification of fault hierarchies is based on three main principles: fault scale, strata penetrated by the fault, and active periods of the fault. Guided by these principles, the AD well area is divided into a three-tier fault system. (1) First-order faults: Active continuously from the Caledonian through the Hercynian to the Yanshanian period. These faults penetrate downward through the T_9^0 interface, are large in scale, and extend almost across the entire study area. Four first-order faults are developed in the AD well area. (2) Second-order faults: Active during the Caledonian and Hercynian periods. These faults penetrate downward through the T_8^0 interface, are relatively large in scale, and terminate at first-order faults. (3)Third-order faults: Formed in the mid-Caledonian period, with little to no activity in the late stage. These are NW or NE trending internal faults within the Ordovician strata, derived from second-order faults. Seismic profiles indicate that first-order faults penetrate downward through T_9^0, have a long activity duration, and extend upward through T_3^4. Second-order faults extend downward to T_8^0, have a moderate activity duration, and terminate upward at the T_5^0 interface. Third-order faults are internal Ordovician faults, active mainly in the early stage and largely inactive in the late stage (Fig.4).

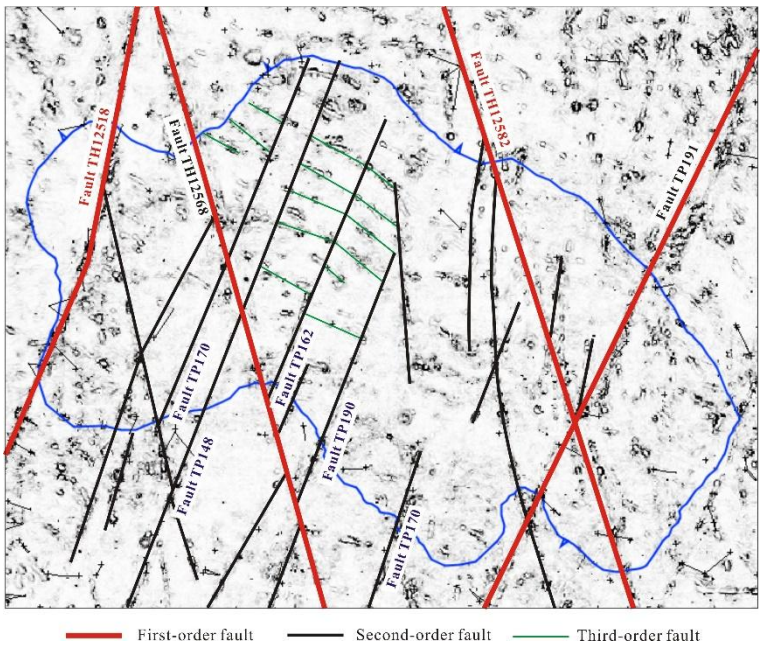


Fig 4. Planar distribution of different-order faults in the AD well area.

4.4 **Fault Charging Characteristics**

Fault strike, fault-Source connectivity, and late-stage fault activity are the three primary factors determining charging intensity. The main hydrocarbon accumulation periods in the Tahe area occurred during the late Hercynian and from the Indosinian to Himalayan stages (Gu 2000). During this time, the maximum principal stress was oriented NE-SW. NE trending faults, whose movement direction aligned with the maximum principal stress, experienced weak normal stress but strong shear stress. Shear-induced dilation promoted the opening of these faults, enhancing their conductivity and facilitating hydrocarbon adjustment and migration. In contrast, NW trending faults were subjected to stronger normal stress, resulting in reduced conductivity due to compressional effects. First-order NE-trending faults, with activity phases well-matched to the accumulation period and excellent source connectivity, exhibit strong charging capacity. The average cumulative production per well drilled in such zones is 96,000 tons. Second-order NE-trending faults, active during the late Hercynian with moderate source connectivity, show intermediate charging capacity, yielding an average cumulative production of 58,000 tons per well. Internal NE-trending faults and poorly connected NW-trending faults have cumulative production below 10,000 tons (table 1).

Table 1. Charging characteristics of faults with different strikes and hierarchies.

Faults		fault penetration capability	Late-stage activity		charging intensity	Average Cumulative Production Per Well (10^4t)
			Late Hercynian period	Indosinian-Himalayan period		
Northeast-trending fault	TH12518 TP191	Penetrate the T90 interface	active	active	Primary charging	9.6
	TP156 TP190 TP170 TP162	Penetrate the T81 interface	active	inactive	Secondary charging	5.8
	Others	Terminates below the T80 interface	inactive	inactive	Tertiary charging	0.3
Northwest-trending fault	TH12568 TH12582	Penetrate the T90 interface	active	active	Primary charging	0.4
	Others	Terminates below the T80 interface	inactive	inactive	Tertiary charging	0.1

5 **Karst Development Characteristics**

The main karstification period in the AD well area was the second phase of the Middle Caledonian orogeny. During this period, surface water systems were well developed in the Lianglitag Formation, with NE and NW trending faults intersecting across the area. Surface water infiltrated downward along these faults, leading to dissolution and the formation of large-scale karst reservoirs. Variations in the distribution of surface drainage systems resulted in differences in karst development patterns between the eastern, central, and western areas. Unconformities of different orders and faults provided pathways for karst water migration, with differential dissolution creating reservoir spaces in both shallow and deep layers. In the eastern and western parts, vertical dissolution was primarily fault-controlled, while the central area exhibited both fault-controlled vertical dissolution and layer-controlled karst conduits (Fig.5a, b). Fracture-cavity systems in shallow layers are relatively discontinuous and mostly scattered, whereas deeper fracture-cavity systems are more developed, showing clear NWW trending distribution with better continuity in local areas. During the formation and evolution of near N-S trending faults, tensile stress concentrated at their tips facilitated the opening of NWW trending

fractures. Under extensional stress conditions, well-developed surface river systems contributed to a high degree of karstification.

The identification of fracture-cavity complexes can effectively guide well location deployment. These complexes, formed by different genetic processes, exhibit characteristic "lateral segmentation and vertical layering. (Fig.5c, d)" In the eastern and western areas, the complexes are delineated based on fault segmentation. For example, the F191 fault is divided into northern and southern segments, corresponding to two distinct complexes. Two wells were deployed in the southern segment, partially draining the reserves, while no wells have been drilled in the northern segment, providing clear guidance for future drilling. Overall, six complexes were identified in the east and three in the west. In the central section, ten complexes were identified based on layered, short karst conduits (Fig.5a).

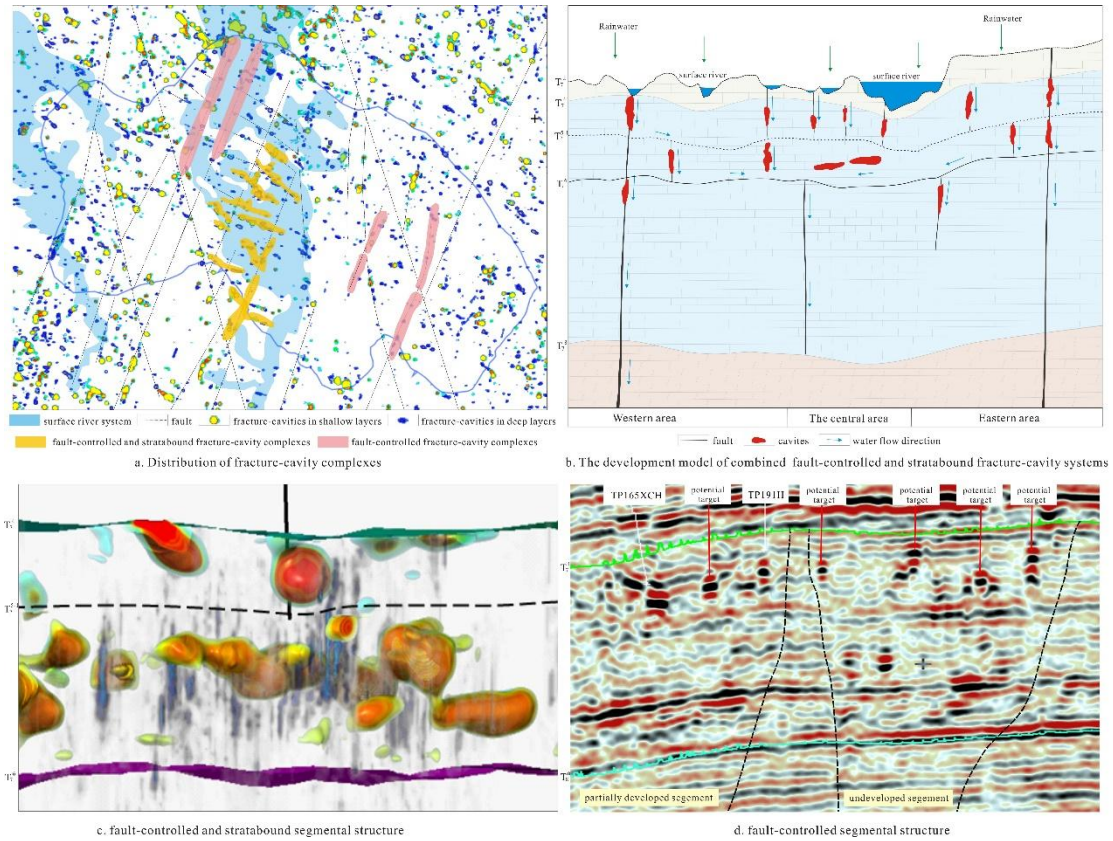


Fig 5. Distribution of fracture-cavity complexes and their segmented, layered structure in the AD well area.

6 **Hydrocarbon Enrichment Models**

Production data from 56 wells in the study area reveal that high-productivity wells are controlled by NE trending hydrocarbon-charging faults. The average cumulative production per well from two large-scale faults is 91,000 tons and 100,000 tons, respectively, while the average cumulative oil production per well from secondary NE-trending faults between them ranges from 30,000 to 70,000 tons. High-productivity wells can be classified into two models: One is located on NE-trending faults that penetrate the T80 interface, with "bead-like" reflections extending up to T_7^4, large-scale fracture-cavity anomalies around the wellbore, and sufficient energy (e.g., Well AD2). the other is situated in zones between NE-trending charging faults, with clear hydrocarbon migration pathways, "bead-like" reflections up to T_7^4, and large-scale fracture-cavity anomalies around the wellbore (e.g., Wells TH12504, TP178). Based on these observations, two enrichment models have been established: (1) Vertical charging and enrichment controlled by NE-trending source-connected faults; (2) Lateral charging and enrichment controlled by secondary faults within the confined zones between major faults (Fig.6).

The appraisal well Th1, drilled in a subtle fault zone in 2024, penetrated 292 meters into the reservoir and produced from both shallow and deep intervals, with an initial production rate of 30 tons of oil per day (Fig.7). This confirms that NE-trending subtle faults possess the ability to charge and adjust hydrocarbons, leading to enrichment in mid-deep layers. This understanding has shifted appraisal targets from conventional secondary fault-controlled areas to subtle fault zones, and expanded development potential from shallow to mid-deep reservoirs. This approach can be applied in the Tahe area, such as the Tuoputai and Block 12 regions, covering geological reserves exceeding 20 million tons.

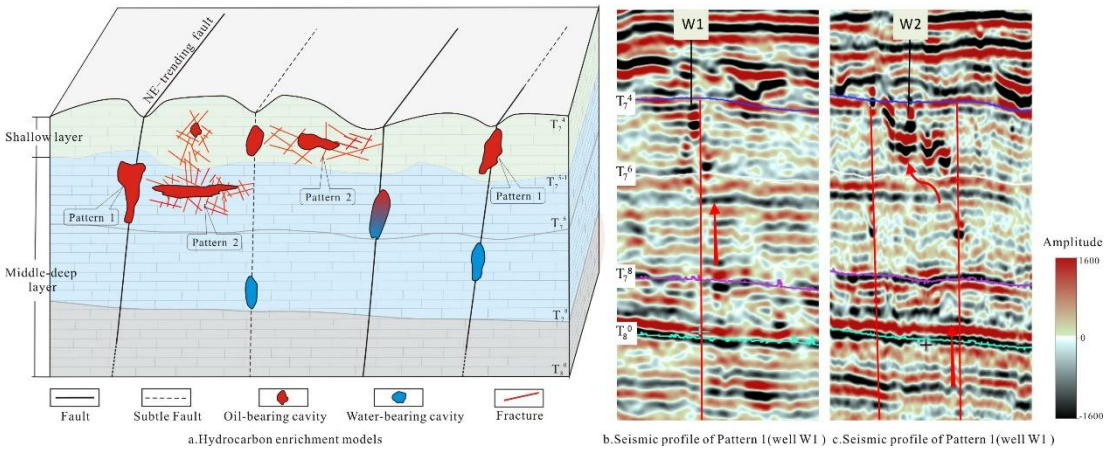


Fig 6. Hydrocarbon enrichment models and typical seismic profiles of drilled wells in the AD well area.

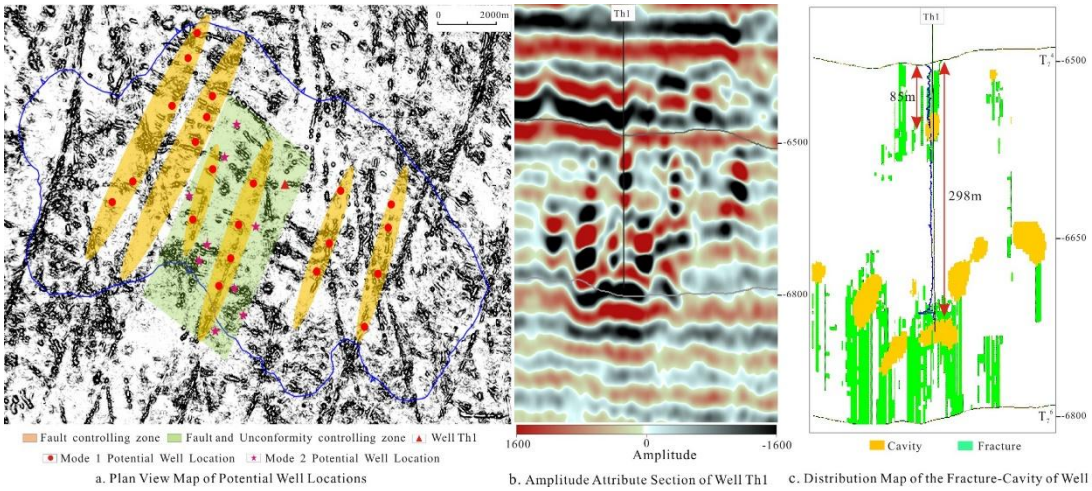


Fig 7. Planar distribution of potential targets and the seismic profile of Well Th1 in the AD well area.

7 Conclusions

(1) Multi-scale processing integrating "time-window integration and azimuth scanning" effectively suppresses high-frequency noise and interference from small fractures and cavities on fault imaging. This enhances the stratigraphic deformation response, revealing subtle, low-order fault zones. As a result, six NE-trending subtle faults were identified in the AD well area.

(2) Controlled by unconformities of different orders and faults, differential dissolution forms reservoir spaces in both shallow and mid-deep layers. In the eastern and western parts, reservoir formation is dominated by fault-controlled vertical dissolution, while the central area exhibits both fault-controlled vertical dissolution and short, layer-controlled karst conduits.

(3) The high-productivity enrichment models in the AD well area are classified into two types: (a) a vertical charging and enrichment model controlled by NE-trending, source-connected faults, and (b) a lateral charging and enrichment model controlled by secondary faults within zones confined between major faults.

(4) Appraisal targets have been expanded from conventional secondary fault-controlled areas to subtle fault zones, and development potential has been extended from shallow to mid-deep reservoirs. This approach can be applied in western Tahe areas such as Tuoputai and Block 12, covering geological reserves of more than 20 million tons.

Acknowledgments

This study was funded by Sinopec Science and Technology Department Project (No. P24220). The author wishes to thank the SINOPEC Northwest Company for supplying various data.

References

Cai J, He YB, Liang JS, Qiu CG, Zhang C (2020) Differential deformation of gravity-driven deep-water fold-and-thrust belts along the passive continental margin of East Africa and their impact on petroleum migration and accumulation. Marine and Petroleum Geology 112: 104053.

Fairhurst B, Ewing T, Lindsay B (2021) West Texas (Permian) Super Basin, United States: Tectonics, structural development, sedimentation, petroleum systems, and hydrocarbon reserves. AAPG Bulletin 105(6): 1099-1147.

Gu Y (2000) Forming Mechanism of Hydrocarbon in Tahe Oilfield of the Northern Tarim Basin. Experimental Petroleum Geology 22(4):307-312.

Li Y, Fan ZH (2011) Developmental pattern and distribution rule of the fracture-cavity system of Ordovician carbonate reservoirs in the Tahe Oilfield. Acta Petrolei Sinica 32:101-106.

Lin T, Tan C, Wang TS, Li QF, Feng MY, Huang SW, Dong JH (2022) Differential hydrocarbon accumulation and its influence on the formation of gas reservoirs in the Longwangmiao Formation, central Sichuan Basin. Petroleum Geology and Experiment 44(4): 655-665.

Liu W, Li YH, Zhang T, LI GR (2002) Study on the sedimentary facies and sequence stratigraphy of the ordovician carbonate rock in Tahe Oilfield. Petroleum Geology & Experiment 24(2):104-109.

Liu SG, Sun W, Zhao YH, Wang GZ, Song LK, Deng B, Liang F, Song JM (2015) Differential accumulation and distribution of natural gas and their main controlling factors in the Upper Sinian Dengying Fm, Sichuan Basin. Natural Gas Industry 35(1):10-23.

Punaova SA, Vinogradova TL (2010) Specifics of the hydrocarbon and trace-element composition of oils and

236 condensates from shallow-water marine deposits. Petroleum Chemistry 50(1): 23-30.

237 Tian J, Wang QH, Yang HJ, Li Y (2021) Petroleum exploration history and enlightenment in Tarim Basin. Xinjiang
238 Petroleum Geology 42(3): 272-282.

239 Zhang K (1999) The discovery of Tahe Oilfield and its geological implication. Oil & Gas geology 20(2):120-124.

240 Zhang S, Jin Q, Qiao Z, Zhang XD, Wei HH, Cheng FQ, Zhu Yj (2020) Differential tectonic evolution of the
241 Ordovician and its significance in petroleum geology in main area of Tahe oilfield. Journal of China University of Mining
242 Technology 49(3):576-586.